Parametrization and smooth approximation of surface triangulations

Michael S. Floater *
Departamento de Matemática Aplicada, Universidad de Zaragoza, Spain
December 1995, revised June 1996

Abstract. A method based on graph theory is investigated for creating global parametrizations for surface triangulations for the purpose of smooth surface fitting. The parametrizations, which are planar triangulations, are the solutions of linear systems based on convex combinations. A particular parametrization, called *shape-preserving*, is found to lead to visually smooth surface approximations.

§1. Introduction

A standard approach to fitting a smooth parametric curve $\mathbf{c}(t)$ through a given sequence of points $\mathbf{x}_i = (x_i, y_i, z_i) \in \mathbb{R}^3$, $i = 1, \ldots, N$ is to first make a *parametrization*, a corresponding increasing sequence of parameter values t_i. By finding smooth functions $x, y, z : [t_1, t_N] \to \mathbb{R}$ for which $x(t_i) = x_i$, $y(t_i) = y_i$, $z(t_i) = z_i$, an interpolatory curve $\mathbf{c}(t) = (x(t), y(t), z(t))$ results. Two commonly used parametrizations are the uniform and chord length ones, in which

$$(t_{i+1} - t_i)/(t_i - t_{i-1}) = 1, \tag{1}$$

and

$$(t_{i+1} - t_i)/(t_i - t_{i-1}) = \|\mathbf{x}_{i+1} - \mathbf{x}_i\|/\|\mathbf{x}_i - \mathbf{x}_{i-1}\|, \tag{2}$$

respectively [2], [6].

In this paper we investigate, by way of numerical examples, a method for making parametrizations for a surface triangulation $\mathcal{S}$ (having triangular facets and a boundary), based on a method proposed by Tutte [25] for making straight line drawings of planar graphs. The nodes $\mathbf{x}_i \in \mathbb{R}^3$ of $\mathcal{S}$ are mapped to points $\mathbf{u}_i = (u_i, v_i) \in D$, for some convex $D \subset \mathbb{R}^2$, in such a way that the image of $\mathcal{S}$ is a planar triangulation $\mathcal{P}$.

The basic idea is to set each $\mathbf{u}_i$ to be a convex combination of its neighbours. By considering certain particular convex combinations, three particular parametrizations are introduced: *uniform*, *weighted least squares*, and *shape-preserving*. The first generalizes (1) and the second and third both generalize (2). The name 'shape-preserving' is chosen because this parametrization has a reproduction property (Proposition 6).

Using a suitable scattered data method [11], smooth functions $x, y, z : D \to \mathbb{R}$, can be constructed independently to satisfy

$$x(\mathbf{u}_i) = x_i, \quad y(\mathbf{u}_i) = y_i, \quad z(\mathbf{u}_i) = z_i. \tag{3}$$

A parametric surface $\mathbf{s} : D \to \mathbb{R}^3$ satisfying $\mathbf{s}(\mathbf{u}_i) = \mathbf{x}_i$ then results from setting

$$\mathbf{s}(\mathbf{u}) = (x(\mathbf{u}), y(\mathbf{u}), z(\mathbf{u})), \qquad \mathbf{u} \in D. \tag{4}$$

* The author was partly supported by the EU project CHRX-CT94-0522.

Though many surface triangulations cannot be mapped into $\mathbb{R}^2$ without considerable deformation, it has been found that surface interpolants $\mathbf{s}$ based on the shape-preserving parametrization are visually smooth. Moreover choosing D to be the unit square and using a two phase method of scattered data approximation [11], the entire surface triangulation can be smoothly approximated by a single tensor-product spline surface $\mathbf{s}'$, a popular surface type in applications.

Most existing methods for approximating surface triangulations fit one or more piecewise polynomial patches to each triangular facet so that the overall geometric continuity is G^k, for some k. Such methods are surveyed by Lounsberry, Mann and DeRose [15]. However this will generate a large amount of data when the number of triangles is high. If the triangulation is a single patch it may be preferable to approximate it with a single parametric surface, for example a tensor-product spline. Milroy et al. [18] have made such approximations directly via a non-linear minimization.

Techniques for mapping and transforming triangulations have been proposed by Maillot et al. [16] and Li et al. [14]. The method in [16] is to minimize an energy functional based on the theory of elasticity, while that in [14] is a numerical approximation, using finite elements or finite differences of elliptic equations.

§2. Graphs and triangulations

We shall draw some standard definitions from graph theory; see [17]. A (simple) graph $\mathcal{G} = \mathcal{G}(V, E)$ is a set of nodes $V = \{i : i = 1, \ldots, N\}$ and a set of edges E, a subset of the set of all unordered pairs of nodes (i, j), $(i \neq j)$. A node j is a *neighbour* of node i if $(i, j) \in E$. The *degree* d_i of the i-th node is the number of its neighbours. A graph $\mathcal{H}$ is a *subgraph* of a graph $\mathcal{G}$ if both its nodes and edges belong to $\mathcal{G}$.

A graph $\mathcal{G}$ is said to be *planar* if it can be embedded in the plane such that

(a) each node i is mapped to a point in $\mathbb{R}^2$,

(b) each edge $(i, j) \in E$ is mapped to a curve whose endpoints are i and j,

(c) the only intersections between curves are at common endpoints.

Such a planar embedding of $\mathcal{G}$ is referred to by Nishizeki [19] as a *plane* graph. A plane graph partitions the plane into connected regions called *faces*. In particular the unbounded face is called the *outer* face. Different embeddings of a planar graph may partition the plane in different ways and this justifies the separate term plane graph.

The subsequent definitions have been chosen to suit the particular applications we have in mind. Let $\mathcal{G}$ be a plane graph and define $\partial\mathcal{G}$ as the subgraph consisting of all nodes and edges which are incident on the outer face. If $\partial\mathcal{G}$ is a simple planar curve then we shall say that $\mathcal{G}$ is *simply connected* and that $\partial\mathcal{G}$ is the *boundary* of $\mathcal{G}$.

We shall say that a plane graph is *triangulated* if all its bounded faces are triangular, i.e. have three edges (no demand is placed on the outer face).

In this paper $\mathcal{G}$ will always be a simply-connected triangulated plane graph, with $N \geq 3$. An example is shown in Figure 1. Though the methods to be discussed can certainly be generalized to a wider range of graphs, including many having faces with more than three edges, this might complicate the exposition unduly and moreover triangulated graphs enjoy some particularly nice properties (see Proposition 4).

We can now describe the triangulations we are interested in.

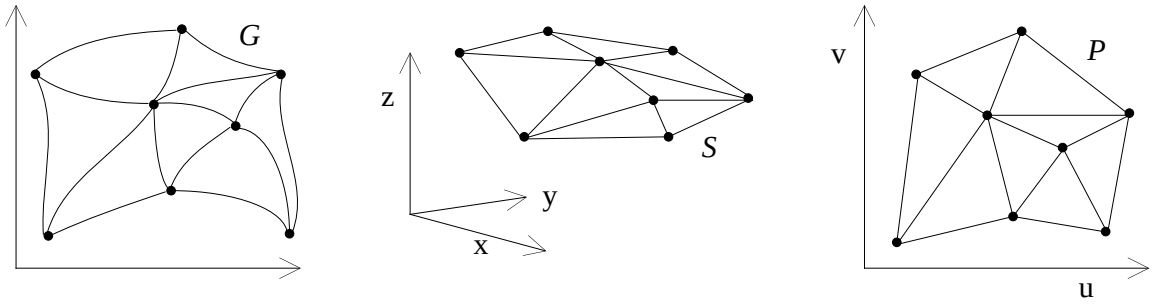

Fig. 1. A graph, a surface triangulation, and parametrization.

Definition 1. *A planar triangulation $\mathcal{P}$ is a simply-connected triangulated plane graph whose edges are straight lines.*

Let F be the set of bounded (triangular) faces of $\mathcal{G}$ and we write $\mathcal{G} = \mathcal{G}(V, E, F)$.

Definition 2. *A surface triangulation $\mathcal{S} = \mathcal{S}(\mathcal{G}, \mathbf{X})$ is an embedding in $\mathbb{R}^3$ of a simply-connected triangulated plane graph $\mathcal{G}(V, E, F)$, $V = \{i : i = 1, \ldots, N\}$, with node set $\mathbf{X} = \{\mathbf{x}_i \in \mathbb{R}^3 : i = 1, \ldots, N\}$, and with straight lines for edges and triangular facets for faces.*

Figure 1 shows an example. We remark that our surface triangulation is less general than the triangulations discussed by Schumaker [23] where the topology can be arbitrary.

§3. Parametrizations

Since the boundary $\partial\mathcal{G}$ of a simply-connected plane graph $\mathcal{G}$ is a simple closed planar curve it has a well-defined orientation, which we will take as the anticlockwise direction.

Definition 3. *Two simply-connected triangulated plane graphs $\mathcal{G}_1$ and $\mathcal{G}_2$ are isomorphic if there is a 1-1 correspondence between their nodes, edges, and faces in a such a way that: corresponding edges join corresponding points; corresponding faces join corresponding points and edges; and the two anticlockwise sequences of nodes in $\partial\mathcal{G}_1$ and $\partial\mathcal{G}_2$ correspond.*

We are now ready to formulate our notion of a parametrization for a surface triangulation; see Figure 1.

Definition 4. *A parametrization of a surface triangulation $\mathcal{S}(\mathcal{G}, \mathbf{X})$ is any planar triangulation $\mathcal{P}$ which is isomorphic to $\mathcal{G}$.*

In this paper we are concerned with finding a parametrization $\mathcal{P}$ for a given surface triangulation $\mathcal{S}$ for the purpose of approximating $\mathcal{S}$ by a smooth parametric surface. We note from Definition 4 that $\mathcal{P}$ need not in general depend on the geometry of $\mathcal{S}$, defined by the points in $\mathbf{X}$. However our numerical examples will demonstrate that in order to approximate $\mathcal{S}$ by a smooth surface, the local geometry of $\mathcal{P}$ ought to mimic the local geometry of $\mathcal{S}$.

Example 1. *Let* $\mathbf{u}_1, \ldots, \mathbf{u}_N$, $N \geq 3$, *be arbitrary pairwise distinct points in* $\mathbb{R}^2$, *not all colinear, and let* $z_1, \ldots, z_N \in \mathbb{R}$ *be arbitrary. Let* $\mathcal{P}$ *be any triangulation, for example the Delaunay triangulation [20], [21], of the* $\mathbf{u}_i$ *and set* $\mathbf{x}_i = (u_i, v_i, z_i)$, *for* $i = 1, \ldots, N$, *where* $\mathbf{u}_i = (u_i, v_i)$. *Then* $\mathcal{P}$ *is a planar triangulation and* $\mathcal{S}(\mathcal{P}, \mathbf{X})$ *is a surface triangulation with parametrization* $\mathcal{P}$.

In Example 1, a natural parametrization $\mathcal{P}$ is provided for approximating $\mathcal{S}$. If $z_i = f(u_i, v_i)$ for some unknown C^1 function $f : \mathbb{R}^2 \to \mathbb{R}$, it is usual to approximate f by a spline function $g : \mathbb{R}^2 \to \mathbb{R}$. Yet, especially if f has steep gradients, a much better result might be obtained by approximating $\mathcal{S}$ and hence the surface $(u, v) \mapsto (u, v, f(u, v))$ by a parametric surface $\mathbf{s} : \mathbb{R}^2 \to \mathbb{R}^3$. This allows the possibility of choosing other parametrizations of $\mathcal{S}$ which may yield smoother surface approximations.

Example 2. *Let* $\mathbf{s} : [0,1] \times [0,1] \to \mathbb{R}^3$ *be a smooth surface and let* $\mathbf{u}_1, \ldots, \mathbf{u}_N$, $N \geq 3$, *be arbitrary pairwise distinct points in* $[0,1] \times [0,1]$, *not all colinear. Let* $\mathcal{P}$ *be any triangulation of the* $\mathbf{u}_i$. *If* $\mathbf{x}_i = \mathbf{s}(\mathbf{u}_i)$, $\mathbf{X} = \{\mathbf{x}_i : i = 1, \ldots, N\}$ *then* $\mathcal{S}(\mathcal{P}, \mathbf{X})$ *is a surface triangulation and* $\mathcal{P}$ *is a parametrization of it.*

We remark that $\mathcal{S}$ in Example 2 need not be injectively projectable onto the plane as in Example 1.

Surface triangulations also arise as crude approximations of various kinds of non-explicit data sets such as cross-sectional data [22], [9] and densely scattered data sampled from three-dimensional objects [13], provided the topology is suitable. In these cases usually no parametrization is available and it is especially important to be able to construct one.

§4. Method for parametrization

Finding any parametrization $\mathcal{P}$ for a given surface triangulation $\mathcal{S}$ can be seen to be equivalent to finding a planar triangulation (with straight line edges) isomorphic to a given triangulated plane graph $\mathcal{G}$. In the language of graph theory this is a matter of constructing a straight line drawing of a plane graph. It was first shown by Fáry [8], using a proof by induction, that every (simple) plane graph has a straight line drawing.

Later, in [24,25], Tutte gave a constructive proof employing a method known as the 'barycentric mapping' for making such a drawing. The boundary nodes of $\mathcal{G}$ are mapped to the boundary of any convex polygon and every internal node in the drawing is defined to be the centre of mass of its neighbours, their barycentre; see Figure 2. The reader is referred to Chiba et al. [3] and Nishizeki [19] for discussions and further methods for constructing straight line drawings of planar graphs.

Tutte's barycentric mapping is the start point for the remainder of this paper. In the following pages we will proceed by

(i) first observing that the barycentric mapping can be made much more general by allowing each internal node to be *any* convex combination of its neighbours, and

(ii) provide an algorithm for choosing the convex combinations so that $\mathcal{P}$ locally preserves the shape of $\mathcal{S}$.

Let $\mathcal{S}(\mathcal{G}, \mathbf{X})$, with $\mathcal{G} = \mathcal{G}(V, E, F)$, be a surface triangulation with node set $\mathbf{X} = \{\mathbf{x}_i = (x_i, y_i, z_i)\}$, $1 \leq i \leq N$. Assume, by relabelling nodes if necessary, that $\mathbf{x}_1, \ldots, \mathbf{x}_n$ are the

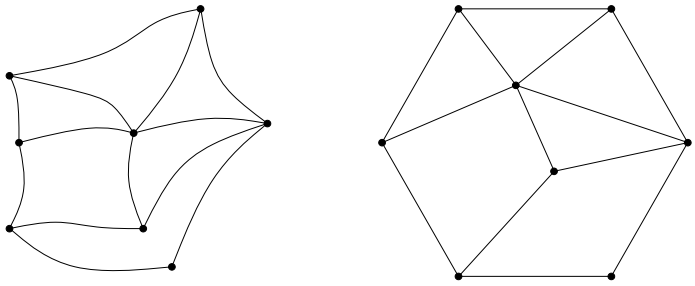

Fig. 2. The barycentric mapping.

internal nodes and $\mathbf{x}_{n+1}, \ldots, \mathbf{x}_N$ are the boundary nodes in any anticlockwise sequence with respect to the boundary of $\mathcal{G}$. Let $K = N - n$. Consider the following definitions.

(1) Choose

$$\mathbf{u}_{n+1}, \ldots, \mathbf{u}_N, \tag{5}$$

to be the vertices of any K-sided convex polygon $D \subset \mathbb{R}^2$ in an anticlockwise sequence.

(2) For each $i \in \{1, \ldots, n\}$, choose any set of real numbers $\lambda_{i,j}$ for $j = 1, \ldots, N$ such that

$$\lambda_{i,j} = 0, \quad (i,j) \notin E, \qquad \lambda_{i,j} > 0, \quad (i,j) \in E, \qquad \sum_{j=1}^{N} \lambda_{i,j} = 1, \tag{6}$$

and define $\mathbf{u}_1, \ldots, \mathbf{u}_n$ to be the solutions of the linear system of equations,

$$\mathbf{u}_i = \sum_{j=1}^{N} \lambda_{i,j} \mathbf{u}_j, \qquad i = 1, \ldots, n. \tag{7}$$

Finally let

$$\mathcal{P} = \mathcal{P}(\mathcal{G}, U_b, \Lambda), \quad \text{with } U_b = \{\mathbf{u}_{n+1}, \ldots, \mathbf{u}_N\}, \text{ and } \Lambda = (\lambda_{i,j})_{i=1,\ldots,n,\ j=1,\ldots,N}, \tag{8}$$

be the embedding of $\mathcal{G}(V, E, F)$ in $\mathbb{R}^2$ with nodes $\mathbf{u}_1, \ldots, \mathbf{u}_n$, straight lines for edges, and triangles for faces.

Note that the equations in (7) demand that every internal point $\mathbf{u}_i$ be a strict convex combination of its neighbours.

We wish to show that $\mathcal{P}$ is a parametrization of $\mathcal{S}$. From Definitions 3 and 4 we see, provided $\mathcal{P}$ is well-defined, that since $\mathcal{P}$ is isomorphic to $\mathcal{G}$, $\mathcal{P}$ is a parametrization provided it is a valid planar triangulation. It is thus only necessary to show that the nodes $\mathbf{u}_i \in \mathcal{P}$ are well-defined, distinct and that no two edges intersect except at common end points.

Tutte [25] was interested in a method of making a straight line drawing of a planar graph. For a large class of plane graphs $\mathcal{G}$, including triangulated ones, he proposed equations (7) in the special case when $\lambda_{i,j} = 1/d_i$ for all $(i,j) \in E$, $i = 1, \ldots, n$ (i.e. $\mathbf{u}_i$ is the barycentre of its neighbours). He proved in this case that they have a unique

solution and that $\mathcal{P}$ is a straight line drawing, that is to say that $\mathbf{u}_1, \ldots, \mathbf{u}_n$ are unique, distinct and no two edges of $\mathcal{P}$ intersect except at common end points. In our case $\mathcal{G}$ is a simply-connected triangulated plane graph. Thus $\mathcal{P}$ is a parametrization of $\mathcal{S}(\mathcal{G}, \mathbf{X})$ whenever $\lambda_{i,j} = 1/d_i$ for all $(i,j) \in E$, $i = 1, \ldots, n$.

We now consider the case of general $\lambda_{i,j}$ in (6). The important thing is to show that (7) has a unique solution. To this end, note that it can be rewritten in the form

$$\mathbf{u}_i - \sum_{j=1}^{n} \lambda_{i,j} \mathbf{u}_j = \sum_{j=n+1}^{N} \lambda_{i,j} \mathbf{u}_j, \qquad i = 1, \ldots, n. \tag{9}$$

By considering the two components u_i and v_i of $\mathbf{u}_i$ separately this is equivalent to the two matrix equations

$$A\mathbf{u} = \mathbf{b}_1, \qquad A\mathbf{v} = \mathbf{b}_2. \tag{10}$$

Here $\mathbf{u}$ and $\mathbf{v}$ are the column vectors $(u_1 \ldots u_n)^T$ and $(v_1 \ldots v_n)^T$ respectively. The matrix A is $n \times n$ having elements

$$a_{i,i} = 1, \qquad a_{i,j} = -\lambda_{i,j}, \quad j \neq i.$$

The existence and uniqueness of a solution to (7) is thus equivalent to the non-singularity of the matrix A. The proof of the following result is based on a proof in [1] of the invertibility of a matrix occuring from a finite difference approximation of Poisson's equation $\Delta u = f$ in two dimensions.

Proposition 1. *The matrix A is non-singular.*

Proof. That A is non-singular is equivalent to the property that the only solution of the equation $Aw = 0$ is $w = 0$ [1]. From (7) the equation $Aw = 0$ can be written as

$$w_i = \sum_{j=1}^{N} \lambda_{i,j} w_j, \qquad i = 1, \ldots, n, \tag{11}$$

where $w_{n+1} = \cdots = w_N = 0$.

Let w_{max} be the maximum of the $w_1, \ldots, w_n$ and suppose that $w_{max} = w_k$. Consider any neighbouring node j of the node k. Since $w_k = w_{max}$ and because of (6), the only way that (11) can be satisfied is if $w_j = w_{max}$. In a similar way every neighbour j of a neighbour of k must satisfy $w_j = w_{max}$ and so on. Eventually, since $\mathcal{G}$ is connected, a boundary node must be reached with the result that $w_j = w_{max}$ for some $j \in \{n+1, \ldots, N\}$. This implies that $w_{max} = 0$. A similar argument shows that $w_{min} = 0$ and therefore that $w = 0$. $\triangleleft$

It remains to show that $\mathcal{P}$ is a triangulation. The proof in [25] that $\mathcal{P}$ is a straight line drawing when $\lambda_{i,j} = 1/d_i$ for $(i,j) \in E$, depends on only one self-explanatory property of barycentres. This property is that if a point $\mathbf{w} \in \mathbb{R}^2$ is the barycentre of any points $\mathbf{w}_1, \ldots, \mathbf{w}_d \in \mathbb{R}^2$ and $\mathbf{l}$ is any line passing through $\mathbf{w}$, then either (a) all the $\mathbf{w}_i$ lie on $\mathbf{l}$ or (b) there is at least one $\mathbf{w}_i$ on either side of $\mathbf{l}$. Since this property evidently still holds when $\mathbf{w}$ is any strict convex combination of its neighbours, the theorem in [25] also applies for the most general $\lambda_{i,j}$ in (6). We conclude as follows.

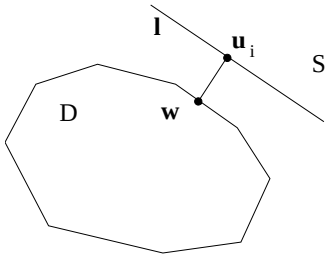

Fig. 3.

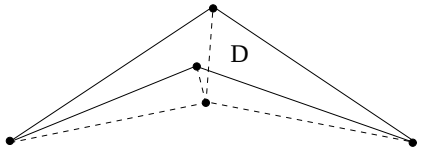

Fig. 4.

Corollary 2. *Let $\mathcal{S}(\mathcal{G}, \mathbf{X})$ be a surface triangulation and let $\mathcal{P} = \mathcal{P}(\mathcal{G}, U_b, \Lambda)$ be an embedding of $\mathcal{G}$ as in (8). Then $\mathcal{P}$ is a parametrization of $\mathcal{S}$.*

The proof in [25] involves a considerable amount of graph theory. We provide here a simple proof that all the internal $\mathbf{u}_i \in \mathcal{P}$ $(i = 1, \ldots, n)$ belong to D, even though it is a consequence of Corollary 2, as it emphasises the importance of the convexity of D.

Proposition 3. *Every internal node $\mathbf{u}_i$ of $\mathcal{P}$, $i \in \{1, \ldots, n\}$, belongs to D.*

Proof. By Proposition 1, $\mathbf{u}_1, \ldots, \mathbf{u}_n$ are well-defined.

To obtain a contradiction suppose that there is at least one internal node of $\mathcal{P}$ not belonging to D. Let $\mathbf{u}_i$ be any such node whose shortest distance to D is maximal and, since D is convex, let $\mathbf{w}$ be the unique point in ∂D nearest to it. The point $\mathbf{w}$ may be either a vertex of D or a point on one of its edges, as in Figure 3.

Passing through $\mathbf{u}_i$ is an infinite line $\mathbf{l}$, perpendicular to the vector $\mathbf{u}_i - \mathbf{w}$. It divides $\mathbb{R}^2$ into two open half spaces and no point $\mathbf{u}_j$ lies in the half space S not containing $\mathbf{w}$.

Now, since $\mathbf{u}_i$ is a strict convex combination of its neighbours and none of them belong to S, they must all lie on $\mathbf{l}$. By the same reasoning, the neighbours of the neighbours of $\mathbf{u}_i$ must lie on this line too, and so on. Eventually, since $\mathcal{G}$ is connected, this implies that a boundary node, which is a point in ∂D, lies on $\mathbf{l}$ which is a contradiction. $\triangleleft$

The convexity of D is also a necessary condition for all solutions of (7) satisfying (6) to belong to D. Even though the single internal node in Figure 4 is a convex combination of its neighbours it nevertheless lies outside D (though not outside the convex hull of D).

The class of parametrizations of the form (8) is very large as we will now see.

Proposition 4. *Let $P(\mathcal{S})$ be the class of all parametrizations, according to Definition 4, of a given surface triangulation $\mathcal{S}$. Define $T(\mathcal{S}) \subset P(\mathcal{S})$ to be those parametrizations of the form (8) and let $C(\mathcal{S}) \subset P(\mathcal{S})$ be those parametrizations whose boundary nodes are the vertices of a convex polygon in an anticlockwise sequence. Then $T(\mathcal{S}) = C(\mathcal{S})$.*

Proof. Due to (5) and Corollary 2, $T(\mathcal{S}) \subset C(\mathcal{S})$. Now suppose $\mathcal{P} \in C(\mathcal{S})$. Then since $\mathcal{P}$ is a planar triangulation, every internal node lies strictly inside the convex hull of its neighbours. Indeed, otherwise one of the faces incident on the node would not be a convex polygon and so could not be a triangle. Consequently every node can be expressed as a strict convex combination of its neighbours, i.e. in the form (7). Since moreover D is a convex polygon, $\mathcal{P} \in T(\mathcal{S})$. $\triangleleft$

Condition (5) demands that $(\mathbf{u}_{i+1} - \mathbf{u}_i) \times (\mathbf{u}_{i+2} - \mathbf{u}_{i+1}) > 0$ for all $i = n+1, \ldots, N$, where we define $(a_1, a_2) \times (b_1, b_2) = a_1 b_2 - a_2 b_1$ and $\mathbf{u}_{N+k} = \mathbf{u}_{n+k}$, for $k = 1, 2$. In the numerical examples we have relaxed this to $(\mathbf{u}_{i+1} - \mathbf{u}_i) \times (\mathbf{u}_{i+2} - \mathbf{u}_{i+1}) \geq 0$. In this way D can be taken to be the unit square, with several boundary nodes lying along each of the four sides. This relaxation caused no problems in practice.

§5. Specific parametrizations

Tutte's barycentric mapping ($\lambda_{i,j} = 1/d_i$, for $(i,j) \in E$) could be regarded as a generalization of uniform parametrization for point sequences. In this section we wish to discuss this and some further specific parametrizations. In order to motivate these, let us review parametrizations for point sequences.

Suppose $\mathbf{X} = \{\mathbf{x}_1, \ldots, \mathbf{x}_N\}$ is a sequence of points in $\mathbb{R}^3$. Then any increasing sequence of values $T = \{t_1 < t_2 < \cdots < t_N\}$ is called a parametrization for $\mathbf{X}$. It is usual to choose t_1 arbitrarily, appropriate positive values $L_1, \ldots, L_{N-1}$, a constant $\mu > 0$, and then define $t_{i+1} = t_i + \mu L_i$ recursively, $i = 1, \ldots, N-1$. For example, when L_i is constant, T is called a uniform parametrization, while if $L_i = \|\mathbf{x}_{i+1} - \mathbf{x}_i\|$ then it is called chord length [6].

It is well known that choosing parameter values by chord length tends to lead to smoother curve approximations than using uniform especially when the data points are unevenly distributed; see Foley and Nielson [10]. For this reason we search for something analogous for surface triangulations. First observe that there are other ways of determining the t_i from the L_i.

Proposition 5. *Suppose $t_1 < t_2 < \cdots t_N$, $t_i \in \mathbb{R}$ and $L_1, L_2, \ldots, L_{N-1} > 0$, $L_i \in \mathbb{R}$. The following statements are equivalent:*

(i) $t_{i+1} = t_i + \mu L_i$, *for* $i = 1, \ldots, N-1$, *some* $\mu > 0$,

(ii) if $s_1 = t_1$, $s_N = t_N$, *then* $t_2, \ldots, t_{N-1}$ *minimize the functional* $F(s_2, \ldots, s_{N-1}) = \sum_{i=1}^{N-1} w_i (s_{i+1} - s_i)^2$, *where* $w_i = 1/L_i$,

(iii) $t_i = \lambda_{i,1} t_{i-1} + \lambda_{i,2} t_{i+1}$, *for* $i = 2, \ldots, N-1$, *where* $\lambda_{i,1} = L_i/(L_{i-1} + L_i)$ *and* $\lambda_{i,2} = L_{i-1}/(L_{i-1} + L_i)$.

Proof. We first show that (ii) implies (iii). Since F is convex, it is minimized when $\partial F/\partial s_i = 0$, for all i. These equations are precisely those in (iii). Conversely, (iii) implies (ii) since the minimum is unique. To see that (i) and (iii) are equivalent, one can easily show that they are both rearrangements of the equation $(t_{i+1} - t_i)/(t_i - t_{i-1}) = L_i/L_{i-1}$. ◁

Thus if L_i is constant, $t_i = (t_{i-1} + t_{i+1})/2$, i.e. t_i is the barycentre of its neighbours. This justifies the term uniform parametrization for $\mathcal{P}$ when $\lambda_{i,j} = 1/d_i$, for $(i,j) \in E$. When $L_i = \|\mathbf{x}_{i+1} - \mathbf{x}_i\|$, Proposition 5 suggests two ways of generalizing the chord length parametrization to surface triangulations: by minimizing squares of lengths of edges as in (ii); and by choosing the $\lambda_{i,j}$ directly in a similar way to (iii). We now briefly consider the first of these, treating the other, which is much more effective, more thoroughly in the next section.

Suppose the boundary points $\mathbf{u}_{n+1}, \ldots, \mathbf{u}_N$ have been chosen and are fixed. Then one could let the internal $\mathbf{u}_i$ be chosen to minimize the functional

$$F(\mathbf{u}_1, \mathbf{u}_2, \ldots, \mathbf{u}_n) = \sum_{(i,j)\in E} w_{i,j}\|\mathbf{u}_i - \mathbf{u}_j\|^2,$$

where $w_{i,j} = w_{j,i} > 0$ for all $(i,j) = (j,i) \in E$. Since $F : \mathbb{R}^{2n} \to \mathbb{R}$ is convex, it has a global minimum which is attained when $\partial F/\partial u_i = \partial F/\partial v_i = 0$ for all i. Since $\|\mathbf{u}_i - \mathbf{u}_j\|^2 = (u_i - u_j)^2 + (v_i - v_j)^2$, we find

$$\frac{\partial F}{\partial u_i} = 2\sum_{j:(i,j)\in E} w_{i,j}(u_i - u_j), \qquad \frac{\partial F}{\partial v_i} = 2\sum_{j:(i,j)\in E} w_{i,j}(v_i - v_j),$$

and consequently, $\mathbf{u}_i = \sum_{j:(i,j)\in E} w_{i,j}\mathbf{u}_j / \sum_{j:(i,j)\in E} w_{i,j}$. This is equivalent to solving (7) with $\lambda_{i,j} = w_{i,j}/\sum_{j:(i,j)\in E} w_{i,j}$. In particular when $w_{i,j}$ is constant for all $(i,j) \in E$, then $\lambda_{i,j} = 1/d_i$. Thus Tutte's barycentric mapping, or uniform parametrization, minimizes the sum of the squares of lengths of edges in $\mathcal{P}$, with respect to a fixed boundary.

Surface approximations were computed based on the parametrizations obtained by setting $w_{i,j} = 1/\|\mathbf{x}_i - \mathbf{x}_j\|^q$, for several values of q including 1. Though the surfaces were generally smoother than when using the uniform parametrization they still suffered from unwanted oscillations. This is probably due to the degrees of freedom being restricted by the condition $w_{i,j} = w_{j,i}$.

§6. Shape-preserving parametrization

The chord length parametrization for a sequence of points $\mathbf{x}_1, \ldots, \mathbf{x}_N \in \mathbb{R}^3$ has the property that if the $\mathbf{x}_i$ lie on a straight line then there is some affine mapping $\phi : \mathbb{R}^3 \to \mathbb{R}^3$ such that $t_i = \phi(\mathbf{x}_i)$ (where we identify t_i with the point $(t_i, 0, 0)$). It is a property of this kind we wish to retain in the bivariate case and we now describe a *shape-preserving parametrization*.

Let $\mathcal{S}(\mathcal{G}, \mathbf{X})$, where $\mathcal{G} = \mathcal{G}(V, E, F)$, be a surface triangulation and suppose that every triangular facet is non-degenerate (has affinely independent vertices). For each i, let $\mathcal{G}_i$ be the subgraph of $\mathcal{G}$ whose nodes are i and its neighbours in $\mathcal{G}$, and whose edges are edges in E which connect pairs of nodes in $\mathcal{G}_i$. Further let $\mathbf{x}_{j_1}, \ldots, \mathbf{x}_{j_{d_i}}$ be the neighbours of $\mathbf{x}_i$ in any anticlockwise sequence, relative to $\mathcal{G}$, and define $\mathbf{X}_i = \{\mathbf{x}_i, \mathbf{x}_{j_1}, \ldots, \mathbf{x}_{j_{d_i}}\}$. Then, referring to Figure 5, our basic idea is to

(i) find a local shape-preserving parametrization $\mathcal{P}_i$ for $\mathcal{S}_i = \mathcal{S}_i(\mathcal{G}_i, \mathbf{X}_i)$, mapping $\mathbf{x}_i$ into $\mathbf{p} \in \mathbb{R}^2$ and $\mathbf{x}_{j_1}, \ldots, \mathbf{x}_{j_{d_i}}$ into suitable $\mathbf{p}_1, \ldots, \mathbf{p}_{d_i} \in \mathbb{R}^2$ and,

(ii) choose $\lambda_{i,j} > 0$, for $j : (i,j) \in E$ to satisfy

$$\mathbf{p} = \sum_{k=1}^{d_i} \lambda_{i,j_k}\mathbf{p}_k, \qquad \sum_{k=1}^{d_i} \lambda_{i,j_k} = 1. \tag{12}$$

Step (i) There are different ways of mapping $\mathcal{S}_i$ into the plane. The obvious approach is to project it onto the least squares plane through $\mathbf{x}_i$ and its neighbours or onto the

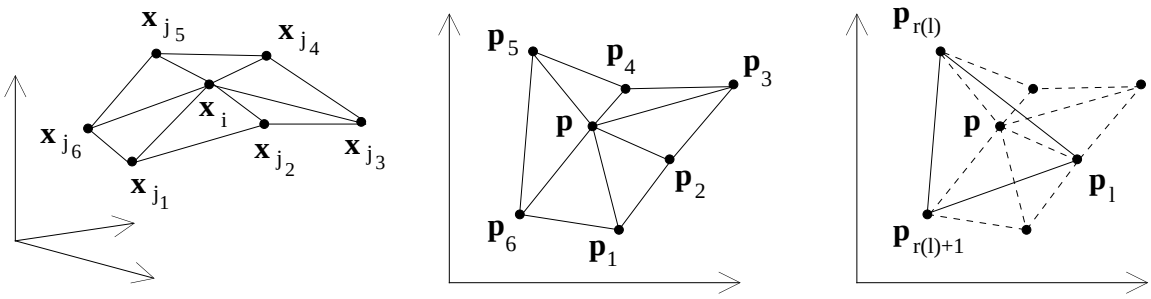

Fig. 5. The subtriangulation $\mathcal{S}_i(\mathcal{G}_i, \mathbf{X}_i)$ and a local parametrization $\mathcal{P}_i$.

plane whose normal is an average of the normals of the triangular facets in $\mathcal{S}_i$. However both these methods can be unstable when there are large angles between the triangular facets in $\mathcal{S}_i$. We have adopted instead a neat method, due to Welch and Witkin [27], for making local parametrizations for surface triangulations which emulates the so-called geodesic polar map, a local mapping known in differential geometry which preserves arc length in each radial direction. The method requires only non-degenerate facets.

Let $\mathrm{ang}(\mathbf{a}, \mathbf{b}, \mathbf{c})$ denote the angle between the vectors $\mathbf{a} - \mathbf{b}$ and $\mathbf{c} - \mathbf{b}$, signed if they are in $\mathbb{R}^2$. Welch and Witkin [27] choose any $\mathbf{p} \in \mathbb{R}^2$ and $\mathbf{p}_1, \ldots, \mathbf{p}_{d_i} \in \mathbb{R}^2$ satisfying, for $k = 1, \ldots, d_i$,

$$\|\mathbf{p}_k - \mathbf{p}\| = \|\mathbf{x}_{j_k} - \mathbf{x}_i\|, \qquad \mathrm{ang}(\mathbf{p}_k, \mathbf{p}, \mathbf{p}_{k+1}) = 2\pi\, \mathrm{ang}(\mathbf{x}_{j_k}, \mathbf{x}_i, \mathbf{x}_{j_{k+1}})/\theta_i, \tag{13}$$

where $\theta_i = \sum_{k=1}^{d_i} \mathrm{ang}(\mathbf{x}_{j_k}, \mathbf{x}_i, \mathbf{x}_{j_{k+1}})$ and $\mathbf{x}_{j_{d_i+1}} = \mathbf{x}_{j_1}$, $\mathbf{p}_{d_i+1} = \mathbf{p}_1$. One can see that $\mathbf{p}$ and $\mathbf{p}_1, \ldots, \mathbf{p}_{d_i}$ are unique up to translations and rotations in $\mathbb{R}^2$. In the implementation we have set $\mathbf{p} = 0$ and $\mathbf{p}_1 = (\|\mathbf{x}_{j_1} - \mathbf{x}_i\|, 0)$ to use up the spare degrees of freedom and then computed $\mathbf{p}_2, \ldots, \mathbf{p}_{d_i}$ in sequence.

Step (ii) The points $\mathbf{p}_1, \ldots, \mathbf{p}_{d_i}$ are the vertices of a star-shaped polygon with $\mathbf{p}$ in its kernel. We now wish to find suitable λ_{i,j_k} satisfying (12). If $d_i = 3$ they are the unique barycentric coordinates of $\mathbf{p}$ with respect to $\triangle \mathbf{p}_1\mathbf{p}_2\mathbf{p}_3$:

$$\lambda_{i,j_1} = \frac{\mathrm{area}(\mathbf{p}, \mathbf{p}_2, \mathbf{p}_3)}{\mathrm{area}(\mathbf{p}_1, \mathbf{p}_2, \mathbf{p}_3)}, \quad \lambda_{i,j_2} = \frac{\mathrm{area}(\mathbf{p}_1, \mathbf{p}, \mathbf{p}_3)}{\mathrm{area}(\mathbf{p}_1, \mathbf{p}_2, \mathbf{p}_3)}, \quad \lambda_{i,j_3} = \frac{\mathrm{area}(\mathbf{p}_1, \mathbf{p}_2, \mathbf{p})}{\mathrm{area}(\mathbf{p}_1, \mathbf{p}_2, \mathbf{p}_3)}. \tag{14}$$

For $d_i > 3$ there is some choice. The following definition has been implemented and yields good results in numerical examples. Regarding Figure 5, for each $l \in \{1, \ldots, d_i\}$, the straight line through $\mathbf{p}_l$ and $\mathbf{p}$ intersects the polygon at a unique second point which is either a vertex $\mathbf{p}_{r(l)}$ or lies on a line segment with endpoints $\mathbf{p}_{r(l)}$ and $\mathbf{p}_{r(l)+1}$. In either case, there is a unique $r(l) \in \{1, \ldots, d_i\}$ and unique δ_1, δ_2, δ_3 such that $\delta_1 > 0$, $\delta_2 > 0$, $\delta_3 \geq 0$, $\delta_1 + \delta_2 + \delta_3 = 1$ and

$$\mathbf{p} = \delta_1 \mathbf{p}_l + \delta_2 \mathbf{p}_{r(l)} + \delta_3 \mathbf{p}_{r(l)+1}.$$

Define $\mu_{k,l}$, for $k = 1, \ldots, d_i$, by $\mu_{l,l} = \delta_1$, $\mu_{r(l),l} = \delta_2$, $\mu_{r(l)+1,l} = \delta_3$, and $\mu_{k,l} = 0$ otherwise. Then for each l we now find

$$\mathbf{p} = \sum_{k=1}^{d_i} \mu_{k,l} \mathbf{p}_k, \qquad \sum_{k=1}^{d_i} \mu_{k,l} = 1, \qquad \mu_{k,l} \geq 0.$$

Finally define

$$\lambda_{i,j_k} = \frac{1}{d_i} \sum_{l=1}^{d_i} \mu_{k,l}, \quad k = 1, \ldots, d_i. \tag{15}$$

Since $\mu_{l,l}$ and $\mu_{r(l),l}$ are non-zero for every l we note that $\lambda_{i,j_k} > 0$ for all k. One also finds that

$$\mathbf{p} = \frac{1}{d_i} \sum_{l=1}^{d_i} \mathbf{p} = \frac{1}{d_i} \sum_{l=1}^{d_i} \sum_{k=1}^{d_i} \mu_{k,l} \mathbf{p}_k = \sum_{k=1}^{d_i} \frac{1}{d_i} \sum_{l=1}^{d_i} \mu_{k,l} \mathbf{p}_k = \sum_{k=1}^{d_i} \lambda_{i,j_k} \mathbf{p}_k,$$

and

$$\sum_{k=1}^{d_i} \lambda_{i,j_k} = \sum_{k=1}^{d_i} \frac{1}{d_i} \sum_{l=1}^{d_i} \mu_{k,l} = \frac{1}{d_i} \sum_{l=1}^{d_i} \sum_{k=1}^{d_i} \mu_{k,l} = \frac{1}{d_i} \sum_{l=1}^{d_i} 1 = 1.$$

Note also that when $d_i = 3$, $r(l) = l + 1$, and

$$\lambda_{i,j_k} = \mu_{k,1} = \mu_{k,2} = \mu_{k,3},$$

and thus (15) conforms with (14). Further, since affine combinations are invariant under translations and rotations, the $\mu_{k,l}$ and therefore the λ_{i,j_k} are uniquely determined by (13) and hence also by $\mathbf{X}_i$. Moreover each λ_{i,j_k} depends continuously (but not smoothly) on $\mathbf{x}_i$ and $\mathbf{x}_{j_1}, \ldots, \mathbf{x}_{j_{d_i}}$. One could also consider taking a weighted average in (15) but this has not been implemented.

The choice of λ_{i,j_k} in (15) provides the following reproduction property. In what follows we identify a point $\mathbf{u} = (u, v) \in \mathbb{R}^2$ with the point $(u, v, 0) \in \mathbb{R}^3$.

Proposition 6. *Suppose that $\mathcal{S}$ is planar and that its boundary nodes $\mathbf{x}_1, \ldots, \mathbf{x}_N$ form a convex polygon in the plane containing $\mathcal{S}$. Let $\mathcal{P}(\mathcal{G}, U_b, \Lambda)$ be a parametrization in which Λ is defined in (15) and such that the boundary points $\mathbf{x}_{n+1}, \ldots, \mathbf{x}_N$ are mapped affinely into $\mathbf{u}_{n+1}, \ldots, \mathbf{u}_N \in U_b$. Then the parametrization $\mathcal{P}$ is an affine mapping of $\mathcal{S}$.*

Proof. Let $\phi : \mathbb{R}^3 \to \mathbb{R}^3$ be the affine mapping for which $\mathbf{u}_i = \phi(\mathbf{x}_i)$ for $i = n+1, \ldots, N$. It is required to show that also $\mathbf{u}_i = \phi(\mathbf{x}_i)$ for $i = 1, \ldots, n$. Using vector and matrix notation we can express ϕ as $\phi(x) = Mx + b$ for some non-singular 3×3 matrix M and vector b, such that the third coordinate of $\phi(x)$ is zero for all x in the plane containing $\mathcal{S}$. Due to (13), since each $\mathcal{S}_i$ is planar, each internal node $\mathbf{x}_i$ and its neighbours are affinely mapped into $\mathbf{p}$ and its neighbours. It follows from (15) that the $\lambda_{i,j}$ satisfy

$$\mathbf{x}_i - \sum_{j=1}^{N} \lambda_{i,j} \mathbf{x}_j = 0, \qquad i = 1, \ldots, n.$$

Therefore,

$$\phi(\mathbf{x}_i) - \sum_{j=1}^{N} \lambda_{i,j} \phi_i(\mathbf{x}_j) = M\mathbf{x}_i + b - \sum_{j=1}^{N} \lambda_{i,j} (M\mathbf{x}_j + b) = M \left(\mathbf{x}_i - \sum_{j=1}^{N} \lambda_{i,j} \mathbf{x}_j \right) = 0.$$

Because the solutions to (7) are unique it follows that $\phi(\mathbf{x}_i) = \mathbf{u}_i$ for $i = 1, \ldots, n$ as required. ◁

The choice of the boundary ∂D should depend on the application and the kind of approximation. If one requires a tensor-product spline approximation the natural choice is the unit square. One could use the unit circle if an approximation in the form of triangular patches or radial basis functions is desirable. When constructing a shape-preserving parametrization, numerical examples have suggested that a good placement of the boundary points $\mathbf{u}_{n+1}, \ldots, \mathbf{u}_N$ around ∂D is by chord length.

§7. Numerical examples

It was found after some experimentation that the matrix equations (10) can adequately be solved by LU decomposition [12] for n up to 500. Beyond that the structure of the matrix A suggests an iterative method would be better.

The matrix A in (10) is diagnonally dominant though not strictly diagonally dominant in any row i if all neighbours of $\mathbf{x}_i$ are internal nodes. It is also sparse but it will not in general be possible to arrange the non-zero entries in a diagonal band structure. This kind of matrix occurs frequently in the numerical solution of differential equations and it was found that an iterative method called Bi-CGSTAB [26] was highly effective. This is a variant of the conjugate gradient method for non-symmetric matrices.

Bi-CGSTAB was used to solve each equation in (10) for n of the order of 25000, setting every internal $\mathbf{u}_i = (u_i, v_i)$ to be a point in the centre of D as an initial guess. The algorithm could be stopped after only a few hundred iterations and no instabilities were experienced. A suitable data structure for the triangulations is that proposed by Cline and Renka [4] for efficient storage of triangulations.

Figure 6 shows a Delaunay triangulation of a set of 27 scattered data points in the plane. The points were mapped uniformly ($\lambda_{i,j} = 1/d_i$ for $(i,j) \in E$) into the unit disc in Figure 7, placing the eight boundary nodes uniformly around the unit circle. In Figure 8, the same points were mapped into the unit square $[0,1] \times [0,1]$. This time four chosen 'corner' boundary points were mapped to the corners of the square and the remaining boundary points mapped uniformly along each side. The points were mapped using the shape-preserving parametrization (15) in Figure 9, the 'sides' being mapped by chord length.

Figure 10 shows a surface triangulation $\mathcal{S}$ of 1000 points sampled from a salt dome, a geological object with an overhang. Three parametrizations $\mathcal{P}$ in the unit square are displayed in Figures 11, 13, and 15, using respectively (i) uniform, (ii) weighted least squares of edge lengths with $w_{i,j} = 1/\|\mathbf{x}_i - \mathbf{x}_j\|$, and (iii) shape-preserving. As in the previous example, four corner points were mapped to the corners of the square, and the sides were mapped uniformly in the first and by chord length in the second two. In each case three C^1 piecewise-cubic interpolants x, y, z, satisfying (3), were then made for each component using the Clough Tocher split on $\mathcal{P}$ [7], [11]. The resulting interpolatory surface $\mathbf{s}(u,v)$, of the form (4) was then sampled on a square 40×40 grid and interpolated by a C^2 cubic tensor-product spline $\mathbf{s}'(u,v)$. These are shown in Figures 12, 14, and 16, respectively. It is very clear that the third surface, based on the shape-preserving parametrization, is visually smoother than the first two.

Finally by retriangulating the $\mathbf{u}_i \in \mathcal{P}$, with a new triangulation $\hat{\mathcal{P}}$, one obtains a new surface triangulation $\hat{\mathcal{S}}$, parametrized by $\hat{\mathcal{P}}$, having the same nodes $\mathbf{x}_i$ as $\mathcal{S}$. If one chooses

$\hat{\mathcal{P}}$ to satisfy some desirable property, this property can be transmitted to $\hat{\mathcal{S}}$, providing an interesting way of 'optimizing' surface triangulations. Such optimizations are usually based on recursively swapping edges in an existing one according to some goodness criterion as described by Schumaker [21], and Dyn, Levin, and Rippa [5].

Moreover replacing $\mathcal{P}$ by $\hat{\mathcal{P}}$ may have a beneficial effect on the surface approximation when it is based on piecewise polynomials on $\hat{\mathcal{P}}$. In Figure 17 the Delaunay triangulation $\hat{\mathcal{P}}$, which maximizes the minimum angle of its triangles, was computed for the $\mathbf{u}_i$ appearing in Figure 15. The tensor-product surface approximation $\hat{\mathbf{s}}'$ of $\hat{\mathcal{S}}$ is displayed in Figure 18. The new surface appears to be somewhat smoother than that in Figure 16, benefitting from more well-proportioned triangles. The corresponding surface retriangulation $\hat{\mathcal{S}}$ is displayed in Figure 19 and it has as might be expected, less long thin triangles than the original in Figure 10. However note that any retriangulation of the parametrization depends on the choice of the boundary.

§8. Final remarks

A method for making shape-preserving parametrizations of surface triangulations has been presented and used to generate well-behaved smooth surface interpolations and approximations.

In this paper $\mathcal{G}$ was assumed to be a triangulated graph. Tutte's barycentric mapping applies to more general graphs, having faces with more than three edges, for example rectangular networks or the graph in Figure 2. With care, the shape-preserving parametrization could similarly be extended to various networks of points in $\mathbb{R}^3$.

Acknowledgement. I wish to thank Hermann Kellermann at SINTEF for help with the implementation of the numerical examples. I am also grateful to Jesús Miguel Carnicer for suggesting improvements to the layout of the paper.

§9. References

1. Atkinson K. E., *An introduction to numerical analysis*, Wiley, new York, 1989.
2. de Boor C., *A Practical Guide to Splines*, Springer-Verlag, New York, 1978.
3. Chiba N., K. Onoguchi, T. Nishizeki, Drawing plane graphs nicely, Acta Informatica **22** (1985), 187–201.
4. Cline A. K., R. L. Renka, A storage-efficient method for construction of a Thiessen triangulation, Rocky Mount. J. Math. **14** (1984), 119–139.
5. Dyn N., D. Levin, S. Rippa, Data dependent triangulations for piecewise linear interpolation, IMA J. Numer. Anal. **10** (1990), 137–154.
6. Farin G., *Curves and surfaces for computer aided geometric design*, Academic Press, San Diego, 1988.
7. Farin G., Triangular Bernstein-Bézier patches, Comp. Aided Geom. Design **3** (1986), 83–128.
8. Fáry I., On straight line representatation of planar graphs, Acta Sci. Math. Szeged **11** (1948), 229–233.
9. Floater M., G. Westgaard, Smooth surface reconstruction from cross-sections using implicit methods, preprint, SINTEF, Oslo.

10. Foley T., G. Nielson, Knot selection for parametric spline interpolation, in *Mathematical Methods in Computer Aided Geometric Design II, T. Lyche and L. Schumaker (eds.), Academic Press, New York, 1992*, 261–271.
11. Franke R., L. Schumaker, A bibliography of multivariate approximation, in *Topics in Multivariate Approximation, C. Chui, L. Schumaker, and F. Uteras (eds.), Academic Press, New York, 1986*, 275–335.
12. Golub G. H., C. F. Van Loan, *Matrix Computations*, John Hopkins Univ. Press, 1989.
13. Hoppe H., T. DeRose, T. DuChamp, J. McDonald, W. Stuetzle, Surface reconstruction from unorganized points, Computer Graphics **26** (1992), 71–78.
14. Li Z., C. Suen, T. Bui, Q. Gu, Harmonic models of shape transformations in digital images and patterns, CVGIP: graph. models and imag. proc., **54** (1992), 198–209.
15. Lounsberry M., S. Mann, T. DeRose, Parametric surface interpolation, IEEE Comp. Graph. and App., (1992), 45–52.
16. Maillot J., H. Yahia, A. Verroust, Interactive texture mapping, SIGGRAPH Comp. Graph. Proc. (1993), 27–34.
17. Marshall C. W., *Applied Graph Theory*, Wiley, New York, 1971.
18. Milroy M., C. Bradley, G. Vickers, D. Weir, G^1 continuity of B-spline surface patches in reverse engineering, Comp. Aided Design **27** (1995), 471–478.
19. Nishizeki T., Planar graph problems, Computing Supplementum **7** (1990), 53–68.
20. Preparata F. P., M. I. Shamos, *Computational geometry*, Springer-Verlag, New York, 1985.
21. Schumaker L. L., Triangulation methods, in *Topics in Multivariate Approximation, C. K. Chui, L. L. Schumaker, F. Utreras (eds.), Academic Press, New York* (1987), 219–232.
22. Schumaker L. L., Reconstructing 3D objects from cross-sections, in *Computation of Curves and Surfaces, W. Dahmen, M. Gasca, and C. Micchelli eds., Kluwer, Dordrecht* (1990), 275–309.
23. Schumaker L. L., Triangulations in CAGD, IEEE Computer Graphics and Applications (1993), 47–52.
24. Tutte W. T., Convex representations of graphs, Proc. London Math. Soc. **10** (1960), 304–320.
25. Tutte W. T., How to draw a graph, Proc. London Math. Soc. **13** (1963), 743–768.
26. van der Vorst H. A., Bi-CGSTAB: A fast and smoothly converging variant of Bi-CG for the solution of nonsymmetric linear systems, SIAMsci, **13** (1992), 631–644.
27. Welch W., A. Witkin, Free-form shape design using triangulated surfaces, Computer Graphics, SIGGRAPH 94 (1994), 247–256.

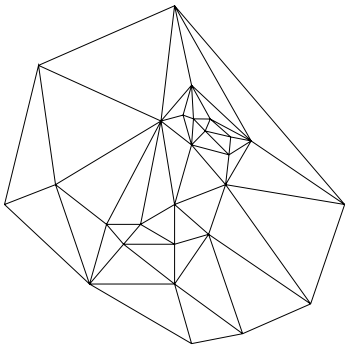

Fig. 6. Delaunay triangulation.

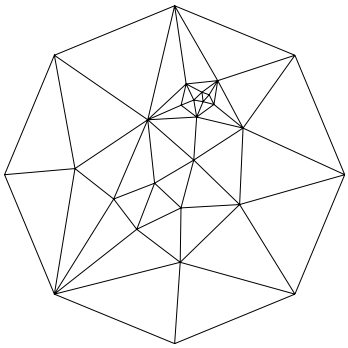

Fig. 7. Uniform parametrization.

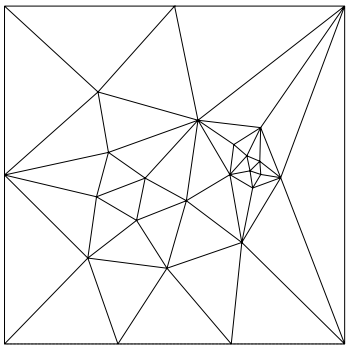

Fig. 8. Uniform parametrization.

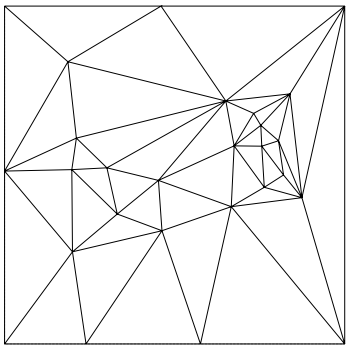

Fig. 9. Shape-preserving parametrization.

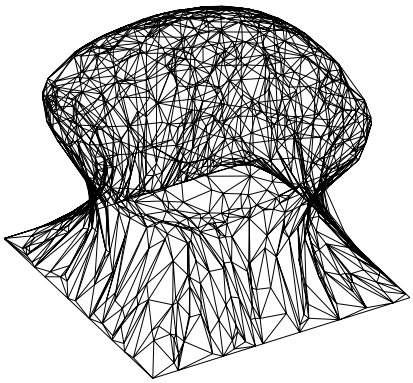

Fig. 10. Triangulated salt dome.

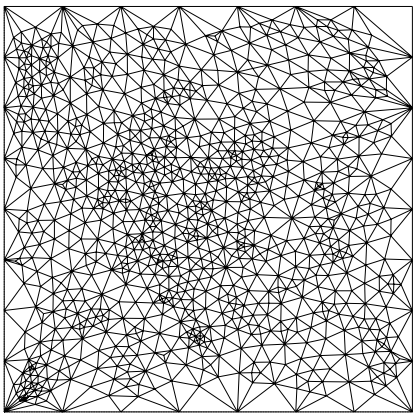

Fig. 11. Uniform parametrization.

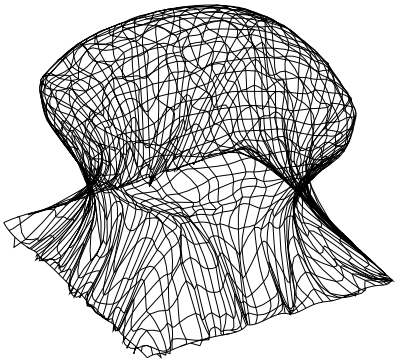

Fig. 12. Surface approximation.

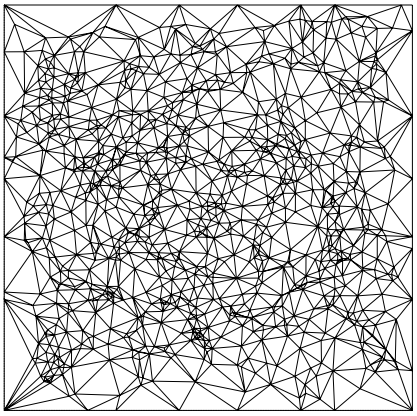

Fig. 13. Weighted least squares parametrization.

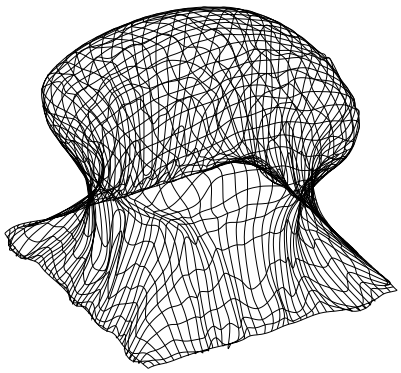

Fig. 14. Surface approximation.

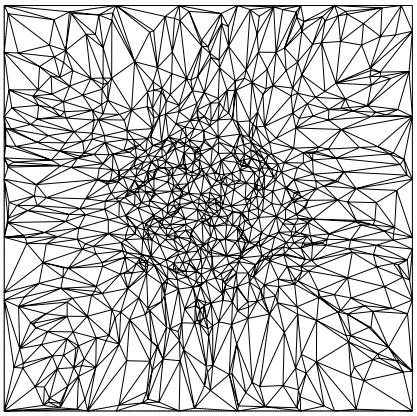

Fig. 15. Shape-preserving parametrization.

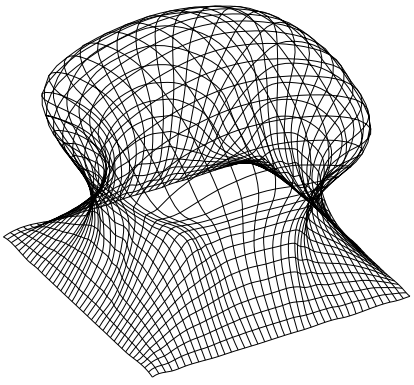

Fig. 16. Surface approximation.

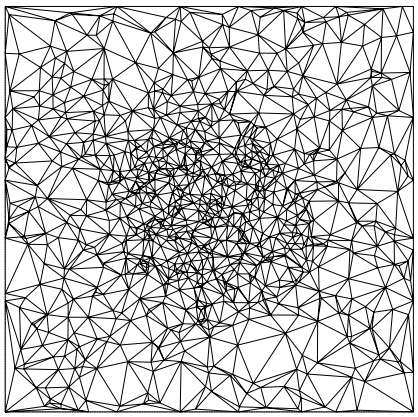

Fig. 17. Delaunay retriangulation.

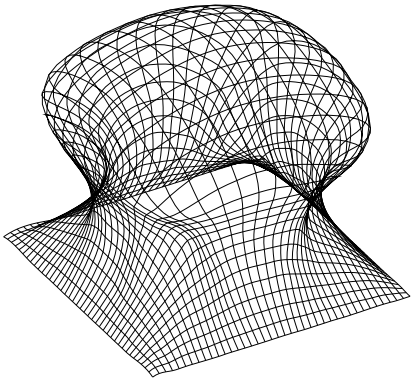

Fig. 18. Surface approximation.

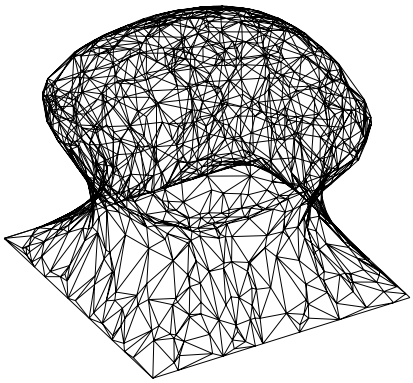

Fig. 19. Surface retriangulation.